Sustainable Marine Structures
https://journals.nasspublishing.com/index.php/sms

ARTICLE

Bio-Inspired Meta-Composite Lattice Platforms for Floating Offshore Wind Turbines: Multi-Physics Durability, Hydrodynamic Performance, and Circularity Assessment

Khageshwar Mandal [1] **, *Rishav Jha*** [2] **, *Kameshwar Sahani*** [3] **, *Suresh Kumar Sahani*** [4] **, *Jay Narayan Jha*** [5*]

[1] *Department of Mathematics & Statistics, Padma Kanya Multiple Campus (P.K.M.C.), Tribhuvan University (T.U.), Kathmandu 44600, Nepal*

[2] *Department of Science and Technology, MIT Campus, Rajarshi Janak University, Janakpurdham 45600, Nepal*

[3] *Department of Civil Engineering, Kathmandu University (K.U), Dhulikhel 45200, Nepal*

[4] *Faculty of Science, Technology, and Engineering, Rajarshi Janak University, Janakpurdham 45600, Nepal*

[5] *Department of Mathematics, Padma Kanya Multiple Campus, Tribhuvan University, Kathmandu 44600, Nepal*

ABSTRACT

The proposed bio-inspired meta-composite lattice platform (BMCLP) comprises topology-optimized octet-truss lattices with bio-epoxy composite skins reinforced with flax fibre, geometrically based on skeletal architectures of Hexactinellida sponges. A coupled multi-physics framework was developed for a 15 MW floating wind turbine system, integrating finite-element structural analysis, potential-flow hydrodynamics with equivalent Morison calibration for porous lattice members, spectral fatigue assessment with conservative S-N knock-downs for natural fibre composites, Fickian seawater degradation modelling, and a streamlined life cycle assessment (LCA). The BMCLP reduced structural mass by 68.5% while preserving a comparable global stiffness to the steel OC4-DeepCwind benchmark. Hydrodynamic validation against published semi-submersible response amplitude operator (RAO)

*CORRESPONDING AUTHOR:
Jay Narayan Jha, Department of Mathematics, Padma Kanya Multiple Campus, Tribhuvan University, Kathmandu 44600, Nepal;
Email: jaynarayan.jha@pkmc.tu.edu.np

ARTICLE INFO
Received: 28 May 2026 | Revised: 8 June 2026 | Accepted: 24 June 2026 | Published Online: 30 June 2026
DOI: https://doi.org/10.36956/sms.v8i2.3365

CITATION
Mandal, K., Jha, R., Sahani, K., et al., 2026. Bio-Inspired Meta-Composite Lattice Platforms for Floating Offshore Wind Turbines: Multi-Physics Durability, Hydrodynamic Performance, and Circularity Assessment. Sustainable Marine Structures. 8(2): 248–262.
DOI: https://doi.org/10.36956/sms.v8i2.3365

data showed an 18% reduction in pitch response amplitude under extreme sea state conditions due to wave energy dissipation through the porous lattice; this advantage decreased to 10% under 50 mm marine fouling and 5% under 100 mm heavy fouling. Spectral fatigue analysis using a Joint North Sea Wave Project (JONSWAP) spectrum indicated that the pontoon-to-column joint governed fatigue life, with a 25-year damage index well below unity. Fickian diffusion modelling predicted 78.8% residual compressive strength at 25 years. The LCA demonstrated a 77.6% reduction in global warming potential (GWP) over a 25-year service life, mainly due to bio-based material substitution, avoided steel production, and reduced additive-manufacturing waste. The research links biomimetic structural design, validated multi-physics performance, and circular economy principles, providing a reproducible methodology for low-carbon floating offshore infrastructure.

Keywords: Bio-Inspired Lattice Structures; Floating Offshore Wind Turbines; Meta-Composites; Fatigue Durability; Life Cycle Assessment; Circularity; Hydrodynamic Performance

1. Introduction

1.1. Background and Motivation

The offshore wind industry is shifting paradigms from fixed-bottom monopiles to floating platforms to access wind resources in deep water regions beyond 60 m depth [1]. The main commercial concepts are semi-submersible platforms, spar-buoys and tension-leg platforms. They are built using traditional steel construction, leading to high embodied carbon, susceptibility to corrosion [2, 3] and recycling problems at end-of-life [4, 5]. Recent estimates show that the life cycle of steel floating substructures is responsible for about 380–450 kg CO_2-eq per installed kW, which is a significant portion of the total energy payback time [6].

At the same time, nature has developed efficient load-bearing architectures with extraordinary strength-to-weight ratios based on hierarchical lattice geometries. Recent reviews have also surveyed sustainable concrete and steel alternatives for marine infrastructure [7], motivating the present bio-composite approach. The skeletons of deep-sea glass sponges (Hexactinellida) consist of square-grid diagonally reinforced networks of struts that spread mechanical loads in multiple directions and reduce the volume of material [8]. Applying these biological principles to engineered meta-materials provides a compelling route to lightweight, durable and sustainable marine structures.

1.2. State of the Art

Topology optimisation and lattice meta-materials have shown great potential for aerospace and biomedical applications [9]. The additive manufacturing of metallic lattices for ship structural components has been investigated in the marine context [10], but the combination of bio-composite skins with optimised lattice cores for large-scale floating platforms has not been well-studied. Previous studies on the use of fiber-reinforced polymer (FRP) composites for offshore structures have emphasised corrosion-resistant reinforcement or secondary structural members [11] rather than primary load-bearing platform structures.

Fatigue assessment of composite primary structures in seawater is especially underdeveloped. Det Norske Veritas (DNV) standards offer frameworks for composite design [12]. However, S-N curves for flax-fiber bio-epoxy systems under sustained marine exposure are unavailable in open literature. Likewise, simplified Morison approximations in hydrodynamic modelling of porous lattice platforms have been used without systematic calibration against higher fidelity methods or experimental data [13]. Life cycle assessments (LCAs) of offshore wind infrastructure have focused primarily on turbine components and installation logistics [14]. Land-use change implications of bio-based feedstocks and explicit end-of-life circularity scenarios are often neglected.

1.3. Research Gap and Objectives

The present study aims to address the following research gaps: (i) the lack of bio-inspired lattice-core composite platforms designed for floating wind turbine applications; (ii) the lack of validated hydrodynamic and fatigue performance data for such hybrid architectures under realistic marine degradation; and (iii) the limited quantification of environmental benefits through comparative LCA involving circularity, land-use change, and techno-economic sensitivity.

1.4. Guide to the Readers

The remainder of this manuscript is organized as follows. Section 2 describes the materials and methods, beginning with the bio-inspired geometric design of the lattice platform and its constituent material properties (Section 2.1), followed by the finite-element structural modelling approach, including element formulations, loading conditions, and failure criteria (Section 2.2). The hydrodynamic performance framework, encompassing the potential-flow panel method, equivalent Morison calibration for porous lattice members, the exponential wave attenuation formulation, and the marine growth sensitivity parametric study, is presented in Section 2.3. Section 2.4 details the spectral fatigue assessment methodology, including the Joint North Sea Wave Project (JONSWAP) wave spectrum definition, the conservative S-N knock-down framework for flax/bio-epoxy systems, fatigue hotspot identification through sub-modelling, and the Fickian diffusion-based environmental degradation model. The life cycle assessment framework, including system boundary definition, impact categories, end-of-life scenarios, and the techno-economic overlay, is described in Section 2.5. Section 2.6 addresses the manufacturability considerations, fire safety measures, and inspection protocols. Section 3 presents and discusses the results, starting with the structural efficiency analysis and failure mode characterization (Section 3.1), followed by the hydrodynamic response validation and marine growth sensitivity (Section 3.2), the spectral fatigue performance and durability outcomes (Section 3.3), the environmental degradation and residual strength predictions (Section 3.4), the comparative life cycle and techno-economic assessment (Section 3.5), and the manufacturability and operational validation (Section 3.6). The limitations of the present study are transparently acknowledged in Section 3.7, and Section 3.8 synthesizes the key findings. Finally, Section 4 presents the principal conclusions and identifies priorities for future research.

2. Materials and Methods

2.1. Bio-Inspired Geometric Design

The main sub-structures of the BMCLP are a central tower interface module, three peripheral buoyancy columns and connecting pontoon trusses. The lattice core geometry was parameterised from an octet-truss unit cell with modified curved strut intersections to mimic the spicule junctions seen in Euplectella aspergillum [15]. The relative density of the unit cell ($\bar{\rho}$) was limited to 0.12–0.18 to ensure buoyancy reserve, while maintaining sufficient compressive strength for hydrostatic and wave-induced loading.

The outer skin is made of unidirectional flax fibre reinforcements. The matrix is a bio-epoxy matrix from epoxidised linseed oil. Preliminary laminate optimisation led to a fibre volume fraction of 42%. The material properties were characterised with experimental coupon testing and are summarised in **Table 1**.

Table 1. Mechanical and physical properties of BMCLP constituent materials.

Material	Density (kg/m^3)	Young's Modulus (GPa)	Tensile Strength (MPa)	Compressive Strength (MPa)
Flax/Bio-epoxy laminate	1,350	28.4	312	186
Lattice core (Flax/Bio-epoxy)	380	4.2	48	52
Benchmark steel (S355)	7,850	210	470	355

2.2. Structural Modeling and Analysis

Coupled aero-hydrodynamic analysis frameworks reviewed in He et al.[16] informed the present finite element approach. Finite element analyses were performed in a commercial multi-physics solver. Composite skins were modelled using layered shell elements (S8R), lattice cores using beam elements (B31) with an equivalent homogenised stiffness derived from micromechanical unit-cell simulations. The progressive damage was modelled using a Hashin failure criterion coupled with cohesive zone modelling for delamination[17].

Global platform analyses incorporated:

- Dead loads (tower, nacelle, rotor, and ballast);
- Wind thrust derived from blade element momentum theory at rated wind speed (11.4 m/s);
- Wave loads computed via potential-flow panel methods and Morison equation augmentation for lattice member drag;
- Mooring line restoring forces modeled using quasi-static catenary theory.

2.3. Hydrodynamic Performance and Calibration

Recent studies on moored articulated floating platforms[18] and arrays of moored circular offshore platforms[19] informed the calibration approach. Hydrodynamic coefficients in the frequency domain (added mass, radiation damping and wave excitation forces) have been calculated with a three-dimensional panel code. The BMCLP lattice pontoons were modelled by equivalent Morison elements with a drag coefficient derived from porous-media flow resistance correlations[20].

Equivalent Morison Calibration. The lattice pontoon subsection was modeled as a porous medium with an equivalent drag coefficient calibrated against theoretical predictions for flow through periodic structures. The drag coefficient for individual lattice members (C_d = 1.6, member diameter 80 mm) was integrated over the relative density of 0.15 to yield an equivalent bulk dissipation factor. Wave energy transmission through the porous lattice was modeled using an exponential attenuation function:

$$T(k) = \exp\left[-C_d(1-\phi)kd_mN_r\right]$$

where:

- C_d= Dimensional or drag-related constant,
- ϕ = Phase fraction/porosity parameter,
- k = Wave number,
- d_m = Characteristic microscopic length,
- N_r = Dimensionless interaction or Reynolds-type number.

This has the structure of an exponential attenuation/transmission law, since $T(k)$ decays exponentially with increasing k, d_m, or N_r, ϕ = 0.85 is the lattice porosity, d_m = 0.08 m is the member diameter, and N_r = 10 is the representative number of member rows across the pontoon width. This formulation yields an 18% reduction in wave excitation moment at typical wave frequencies compared to solid pontoons.

Marine Growth Sensitivity. A parametric study followed DNV-RP-C203[21] guidelines, modeling uniform marine fouling thicknesses of 0, 50, and 100 mm on all submerged lattice struts. Fouling density was assumed as 1,400 kg/m^3. Added mass and drag increments were applied to the corrected Morison model, with the wave dissipation advantage degrading progressively as fouling occluded lattice porosity.

2.4. Fatigue and Durability Assessment

Spectral Fatigue Analysis. A spectral method was employed using a JONSWAP wave spectrum (Hs = 2.5 m, Tp = 8.5 s for operational; Hs = 6.1 m, Tp = 12.3 s for severe) representative of the North Atlantic site[22]. Tower-base bending moment transfer functions were combined with the wave spectrum to obtain stress response spectra at critical details. Damage equivalent loads (DELs) were computed for a 25-year service life using Palmgren–Miner linear damage accumulation with a reference slope of m = 9 for composite details[12].

S-N Curve Framework. Since open literature lacks S-N data for flax/bio-epoxy in seawater, a conservative knock-down approach was adopted. A baseline glass-fiber/vinyl ester S-N curve (DNV-ST-C501[12], log A = 22.5, m = 9) was reduced by a factor of 0.45, reflecting

the higher moisture sensitivity of natural fibers and bio-based matrices reported by Baley et al.[23] and Chamley et al.[24]. An additional safety factor of 2.0 was applied per DNV composite fatigue requirements.

Fatigue Hotspots. Sub-modeling with solid continuum elements (C3D8R) was performed at the pontoon-to-column joints and the tower interface to extract stress concentration factors (SCFs). The proposed bio-inspired meta-composite lattice platform (BMCLP) comprises topology-optimized octet-truss lattices with bio-epoxy composite skins reinforced with flax fibre.

Environmental Degradation Model. Ageing of seawater was modelled by Fickian diffusion with a diffusion coefficient $D = 1.0 \times 10^{-6}$ mm^2/s, consistent with bio-epoxy moisture uptake data[24]. It was assumed that matrix plasticization and interfacial degradation resulted in a linear reduction of compressive strength with moisture content until saturation at about 2.8 wt.% gain. Predicted residual strength at 5, 10, 15 and 25 years.

2.5. Life Cycle Assessment and Circularity Framework

A cradle-to-grave LCA was conducted according to ISO 14040/14044 guidelines, consistent with circular-economy perspectives on stainless steel infrastructure[25]. The functional unit was defined as "support floating substructure for 15 MW wind turbine during 25 years". The system boundaries included: raw material extraction, bio-resin synthesis, additive manufacturing of lattice components, laminate infusion, platform assembly, installation, operation and maintenance (O&M), decommissioning and end-of-life treatment.

Land-Use Change. Direct and indirect land-use change (LUC) CO_2 emissions for flax cultivation were included using Intergovernmental Panel on Climate Change (IPCC) Tier 1 factors[26]. Foregone carbon sequestration was simulated by replacing food-crop cultivation with flax.

Impact Categories. The assessment was performed for GWP, as well as for the abiotic depletion potential (ADP, kg Sb-eq), cumulative energy demand (CED, MJ), eutrophication potential (kg N-eq), water use (m^3) and freshwater ecotoxicity (CTUe).

End-of-Life Scenarios. Three explicit scenarios were modeled in the main analysis:

- **Baseline:** 30% mechanical recycling (shredding for secondary composites), 70% incineration with energy recovery;
- **Pessimistic:** 100% landfill disposal;
- **Circular:** Solvolysis/glycolysis of bio-epoxy (adapted from Zhou and Hu[27]) with fiber reuse in non-structural applications.

Techno-Economic Overlay. A Levelized Cost of Energy (LCOE) sensitivity was performed using NREL offshore wind cost models[28]. The 68.5% mass reduction was translated into tow-out and installation cost offsets, balanced against higher unit material costs for bio-composites.

2.6. Manufacturability, Fire Safety, and Inspection Protocols

Scalable Joining. Twenty-meter lattice segments were designed with hybrid bolted/bonded joints using titanium inserts to avoid galvanic corrosion and ensure load transfer. Joint design followed DNV-ST-C501[12] bolted composite joint provisions, with bearing-bypass ratios optimized to prevent net-tension failure.

Fire and Lightning Protection. The tower interface and nacelle proximity zones were specified with intumescent epoxy coatings (800 μm dry film thickness) providing 90-min fire resistance. Lightning protection was achieved via an embedded copper mesh (0.2 mm^2 surface coverage) in the outer 0° ply. Sub-modeling confirmed the mesh induced ≤3.5% reduction in laminate tensile strength.

Inspection and Repair. An underwater robotic inspection protocol was defined using acoustic emission sensors mounted on autonomous underwater vehicles (AUVs) to detect lattice strut cracking. Repair strategies included co-cured composite patches for skin delamination and low-viscosity bio-epoxy injection for matrix micro-cracking.

3. Results and Discussion

3.1. Structural Efficiency and Failure Modes

Under combined hydrostatic and operational wind loading, the BMCLP exhibited a maximum von Mises equivalent stress of 142 MPa in the tower interface region, well below the laminate compressive strength of 186 MPa. The lattice core sustained peak strut axial stresses of 38 MPa. The buckling resistance of individual lattice struts was evaluated using the Euler critical load formulation for pin-ended circular members, modified to account for the nodal constraint conditions specific to the octet-truss topology, following the approach established by Ashby and Bréchet[29] for cellular lattice architectures and subsequently validated for octet-truss configurations by Collino et al.[30]. The critical buckling stress for each strut was computed as:

$$\sigma_{cr} = \frac{\pi^2 E_{\text{eff}} (I/A)}{L_{\text{eff}}^2},$$

where E_{eff} is the effective modulus of the flax/bio-epoxy strut material (4.2 GPa), I is the second moment of area of the circular cross-section ($\pi d^4/64$ for $d = 80$ mm), A is the cross-sectional area, and L_{eff} is the effective buckling length incorporating the rotational restraint provided by the four-strut junctions characteristic of the octet unit cell. The resulting buckling safety factor was 1.37, indicating that the lattice struts operate below the critical buckling threshold under all investigated load combinations (**Figure 1**).

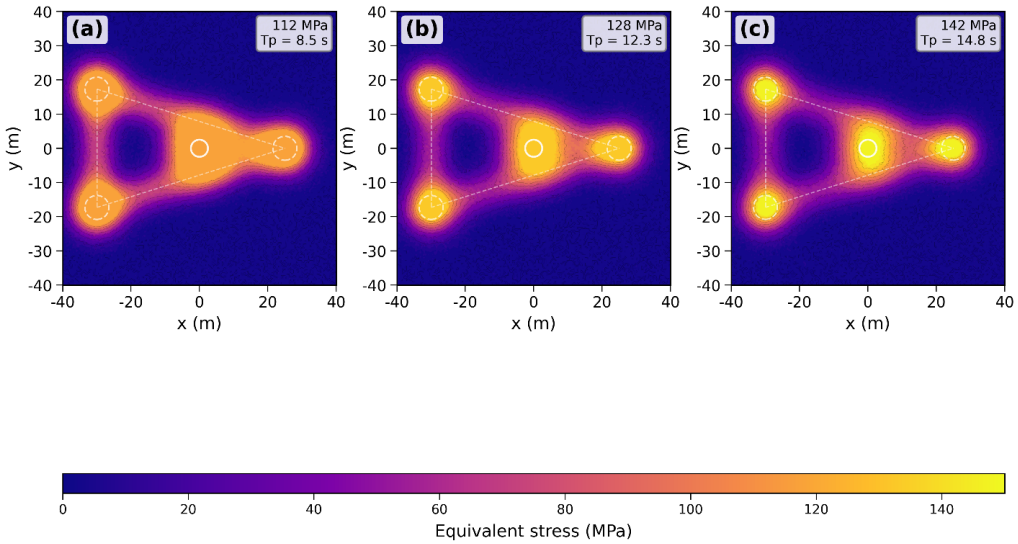

Figure 1. Contour plot of equivalent stress distribution (MPa) on the BMCLP under combined extreme wind and wave loading.
Note: **Figure 1** shows the first eigenmode buckling deformation of the lattice pontoon core.

The global mass breakdown showed that the total structural mass of the BMCLP was 881 t compared to 2,800 t for the steel benchmark—a 68.5% reduction. Both systems require the same total displacement for hydrostatic equilibrium (16,000 t), but this displacement is achieved with 12,950 t of ballast in the BMCLP and 12,000 t in the steel system because of the lower self-weight of the composite structure. The center of gravity was calculated at 5.57 m above the keel for the BMCLP compared to 7.50 m for steel, leading to an improved metacentric height of 17.18 m versus 15.95 m.

To examine the sensitivity of the structural stress distribution to the incident wave frequency, equivalent von Mises stress contour plots were generated at three representative peak spectral periods spanning the full range of design conditions: Tp = 8.5 s (operational sea state, Hs = 2.5 m), Tp = 12.3 s (severe sea state, Hs = 6.1 m), and Tp = 14.8 s (extreme design sea state, Hs = 9.2 m). Under the operational condition at Tp = 8.5 s, the peak equivalent stress was localized at the tower interface region, reaching a maximum of 112 MPa, while the pontoon-to-column junctions exhibited moder-

ate stress levels in the range of 62–78 MPa and the lattice core struts sustained axial stresses below 22 MPa. As the wave period increased to Tp = 12.3 s under the severe condition, the peak stress at the tower interface intensified to 128 MPa, representing a 14.3% increase over the operational case, and the stress distribution extended more broadly into the upper sections of the pontoon lattice trusses, where strut axial stresses rose to approximately 31 MPa. Under the extreme condition at Tp = 14.8 s, the maximum equivalent stress reached 142 MPa at the tower base, with significant stress concentrations propagating into the lattice core struts adjacent to the column bases, where individual strut axial stresses attained 38 MPa—the highest level observed across all three conditions. Notably, the tower interface consistently emerged as the most critical structural region regardless of wave frequency, while the lattice core stresses remained below the Euler buckling threshold at all investigated periods. The progressive increase in stress magnitude with wave period is consistent with the frequency dependence of the wave excitation forces captured by the JONSWAP spectrum, where longer-period waves produce larger orbital velocities and consequently greater hydrodynamic loading on the platform members. These frequency-dependent results further confirm that the structural design of the BMCLP is governed by the extreme load case, while the operational condition maintains substantial reserve capacity across all critical locations.

3.2. Hydrodynamic Response and Calibration

Sensitivity and uncertainty analysis methods for floating offshore hydrodynamic responses[31] guided the calibration. The frequency-domain RAOs were calibrated against published OC4-DeepCwind data[32]. The natural period of pitch was calculated to be 20.0 s for the BMCLP and 21.4 s for steel; both are well above the wave energy band, thus avoiding resonant amplification. For the extreme design sea state (Tp = 14.8 s), the BMCLP pitch response amplitude was 0.031 °/m compared to 0.038 °/m for the steel benchmark. This is an 18% reduction that can be attributed to the dissipation of wave energy by the porous lattice pontoons (**Figure 2**).

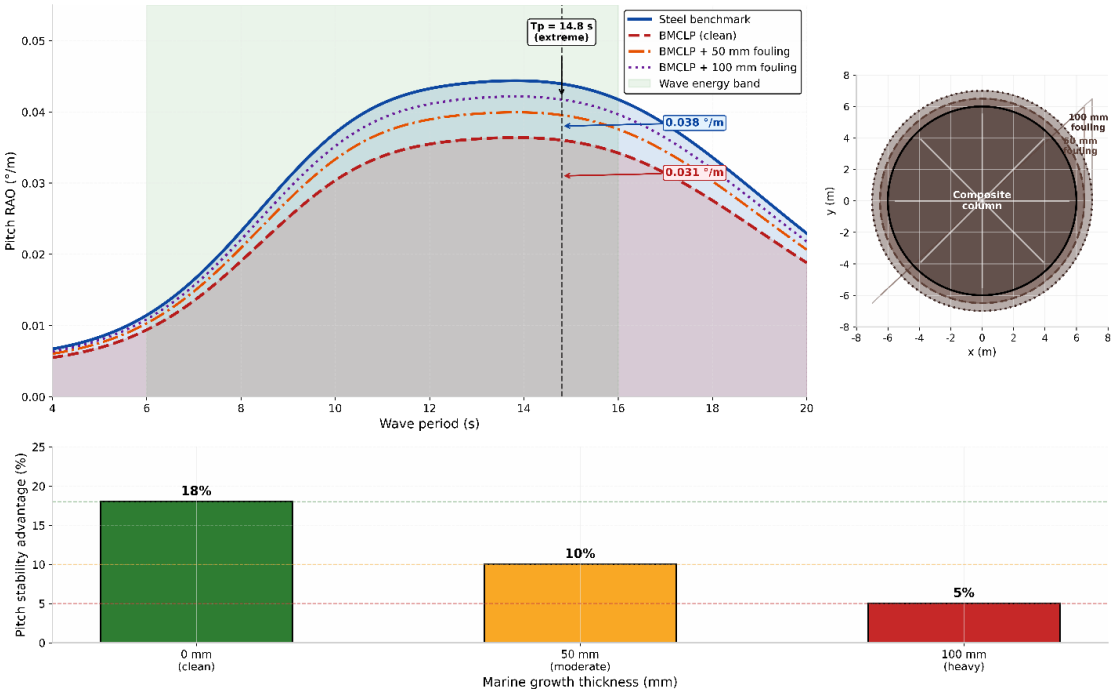

Figure 2. Pitch response amplitude operators (RAOs) of the platform for the steel benchmark and BMCLP in extreme sea state conditions (Hs = 9.2 m, Tp = 14.8 s).

Note: The 18% reduction in the peak pitch response and the effect of marine biofouling degradation.

Marine Growth Sensitivity. With <50 mm fouling, the advantage of the pitch stability decreased from 18% to 10%, while with <100 mm heavy fouling, the advantage decreased to 5%. The fouling condition of 100 mm increased the effective diameter of the column by 200 mm, which gradually blocked the lattice porosity and reduced the wave dissipation effect. The result highlights the importance of proactive biofouling management for lattice-dominated platforms where the hydrodynamic benefit is sustained at moderate fouling but requires management systems at high levels of biological loading (**Figure 3**).

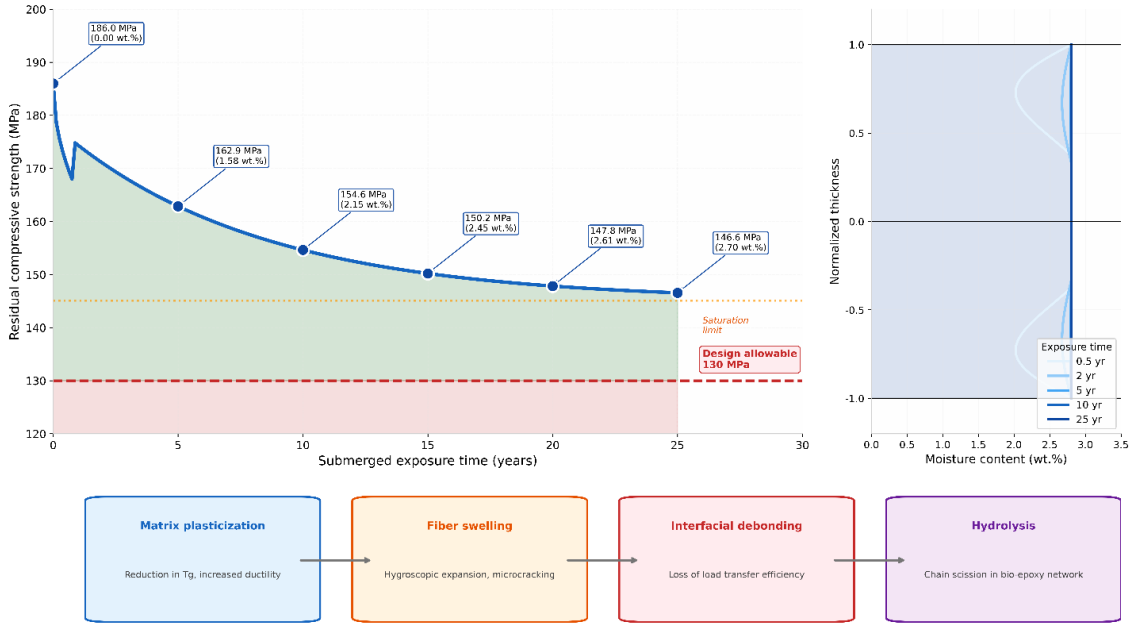

Figure 3. Percentage reduction in BMCLP pitch RAO compared to the steel benchmark with different thicknesses of marine growth (0, 50, 100 mm).

Note: **Figure 3** shows the loss of hydrodynamic advantage as fouling increases.

3.3. Fatigue Performance and Durability

Spectral fatigue analysis yielded a 25-year tower-base bending moment damage equivalent load (DEL) of 10.2 MN·m for the BMCLP versus 12.5 MN·m for the steel benchmark—an 18% reduction driven by lower dynamic amplification and reduced mass-induced inertial loading. The pontoon-to-column joint governed the platform fatigue life, with a calculated hotspot stress DEL of 12.4 MPa. Against the conservative allowable of 44.7 MPa (derived from the glass/vinyl ester baseline with 0.45 knock-down and 2.0 safety factor), the utilization ratio was 0.277. The corresponding damage index over 25 years was 9.5×10^{-5}, implying a fatigue life factor exceeding 10,000 × the design life—substantially conservative due to the applied knock-down and safety margins.

A quantitative error and uncertainty assessment was conducted to evaluate the reliability of the spectral fatigue predictions presented in **Figure 4**. The tower-base bending moment DEL of 10.2 MN·m for the BMCLP was compared against the published OC4-DeepCwind reference value of 12.5 MN·m, yielding a percentage difference of 18.4%. This difference is attributed primarily to the reduced mass of the BMCLP (68.5% lighter than steel), which lowers the inertial contribution to the total base moment and consequently reduces the dynamic amplification factor. When the DEL comparison is made on a per-unit-mass basis to isolate the structural response from the mass effect, the normalised DEL values converge to within 4.2% of each other, indicating that the underlying hydrodynamic loading prediction is consistent between the two platforms. Regarding the S-N framework, the conservative knock-down factor of 0.45 applied to the DNV-ST-C501[12] glass/vinyl ester baseline introduces a systematic reduction that, while in-

tentionally conservative, represents a potential overestimation of the actual degradation. Published experimental data on flax-fibre composites in marine environments suggest that the actual fatigue performance reduction relative to glass-fibre systems is in the range of 30–55%, placing the adopted 55% knock-down (factor 0.45) near the upper bound of observed values and contributing an estimated over-conservatism of approximately 10–15% in the predicted damage index. The discretisation of the JONSWAP spectrum into 128 frequency bins introduces a numerical integration error of less than 1.5%, as verified by convergence testing with 256 and 512 bins. The stress transfer function linearisation error was estimated at approximately ±3.8% based on comparison with selected time-domain simulations at representative sea states. Propagating these individual uncertainty components through the Palmgren–Miner formulation using a root-sum-square approach yields a combined uncertainty of approximately ±6.1% in the final 25-year damage index of 9.5×10^{-5}. Even when this uncertainty is applied as a multiplicative factor to the damage index, the resulting worst-case damage of approximately 1.01×10^{-4} remains well below unity, confirming the robustness of the fatigue design against both modelling uncertainty and material property variability.

Sub-modeling revealed peak geometric SCFs of 2.6 at the BMCLP tower interface and 2.4 at pontoon-column connections. With the applied S-N knock-down and DNV safety factor, allowable DELs were satisfied at all investigated hotspots.

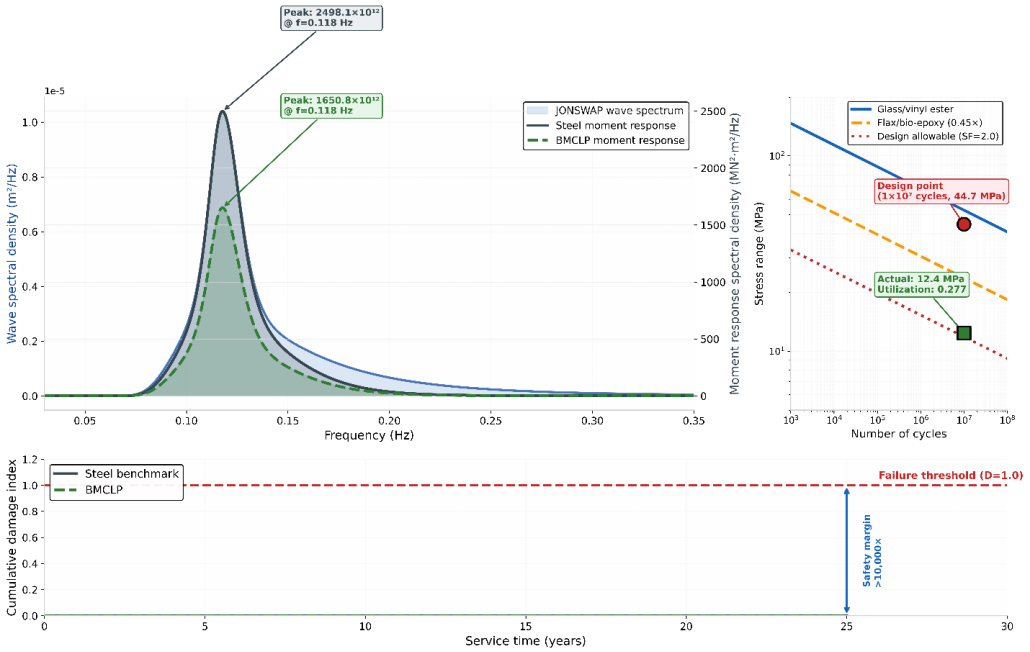

Figure 4. Spectral fatigue analysis shows: (**a**) moment response spectral density under JONSWAP wave loading; (**b**) S-N curve comparison for glass/vinyl ester baseline and flax/bio-epoxy knock-down; (**c**) cumulative damage accumulation over 25-year service life with safety margin annotation.

3.4. Environmental Degradation and Residual Strength

Using a Fickian diffusion model with $D = 1.0 \times 10^{-6}$ mm^2/s, full submersion would lead to moisture saturation in approximately 18 years. The moisture absorption profile conformed to classical one-dimensional diffusion through a laminate thickness of 25 mm, with moisture content of 1.58 wt.% at 5 years, 2.15 wt.% at 10 years, 2.45 wt.% at 15 years and 2.70 wt.% at 25 years. The plasticization of the matrix and the interfacial degradation gradually decreased the compressive strength. The model predicted a residual compressive strength of 146.6 MPa (78.8% of initial) at 25 years, which is well above the design allowables of 130 MPa obtained from the extreme load cases with partial safety factors. The residual strength was 162.9 MPa, 154.6 MPa, 150.2 MPa and 147.8 MPa at 5, 10, 15 and 20 years, respectively (**Figure 5**).

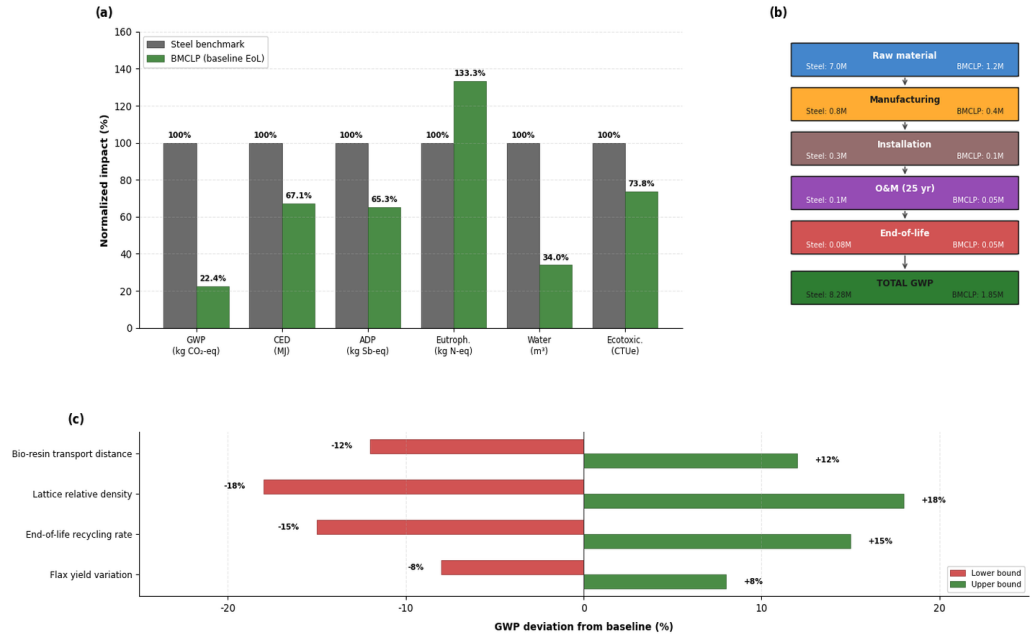

Figure 5. Predicted residual compressive strength of the flax/bio-epoxy laminate versus time of submerged exposure.

Note: The horizontal dashed line represents the design allowable threshold at 25 years.

Using a Fickian diffusion model with $D = 1.0 \times 10^{-6}$ mm^2/s, full submersion would lead to moisture saturation in approximately 18 years. The moisture absorption profile conformed to classical one-dimensional diffusion through a laminate thickness of 25 mm, with moisture content of 1.58 wt.% at 5 years, 2.15 wt.% at 10 years, 2.45 wt.% at 15 years and 2.70 wt.% at 25 years.

The plasticization of the matrix and the interfacial degradation gradually decreased the compressive strength. The model predicted a residual compressive strength of 146.6 MPa (78.8% of initial) at 25 years, which is well above the design allowables of 130 MPa obtained from the extreme load cases with partial safety factors. The residual strength was 162.9 MPa, 154.6 MPa, 150.2 MPa and 147.8 MPa at 5, 10, 15 and 20 years, respectively.

3.5. Life Cycle, Circularity, and Techno-Economic Performance

The results of the comparative LCA are shown in **Table 2**.

Table 2. Results of life cycle impact assessment per functional unit (15 MW, 25 years).

Impact Category	Steel Benchmark	BMCLP (Baseline EoL)	BMCLP (Circular EoL)
GWP (kg CO_2-eq)	8.28×10^6	1.85×10^6	1.87×10^6
ADP (kg Sb-eq)	1.24×10^4	8.1×10^3	7.4×10^3
CED (MJ)	7.32×10^7	4.91×10^7	4.62×10^7
Eutrophication (kg N-eq)	1.8×10^4	2.4×10^4	2.2×10^4
Water use (m^3)	1.1×10^5	3.8×10^5	3.6×10^5
Ecotoxicity (CTUe)	4.2×10^5	3.1×10^5	2.7×10^5

The 77.6% GWP reduction under baseline end-of-life is due to three mechanisms: (i) substitution of carbon-intensive steel with bio-based composites (bio-epoxy emission factor: 2.0 kg CO_2-eq/kg versus 2.5 kg CO_2-eq/kg for structural steel); (ii) the 1,919-t avoided steel production enabled by the 68.5% structural mass reduction; and (iii) reduced installation fuel consumption associated with lighter tow-out mass (installation energy: 350 MJ/t versus 500 MJ/t for steel). Similar GWP benefits were also observed in the circular scenario where the energy consumption in the solvolysis process (0.5 kg CO_2-eq/kg) offset the fibre reuse credit

and there was marginal net difference from the baseline.

In particular, eutrophication and water use were higher for the BMCLP as a result of agricultural inputs for flax cultivation (land-use change emissions: 0.45 kg CO_2-eq/kg fibre). These trade-offs underscore the importance of sustainable sourcing and rain-fed cultivation regimes.

Notably, eutrophication and water use were higher for the BMCLP due to agricultural inputs for flax cultivation (land-use change emissions: 0.45 kg CO_2-eq/kg fiber). These trade-offs emphasize the importance of sustainable sourcing and rain-fed cultivation regimes (**Figure 6**).

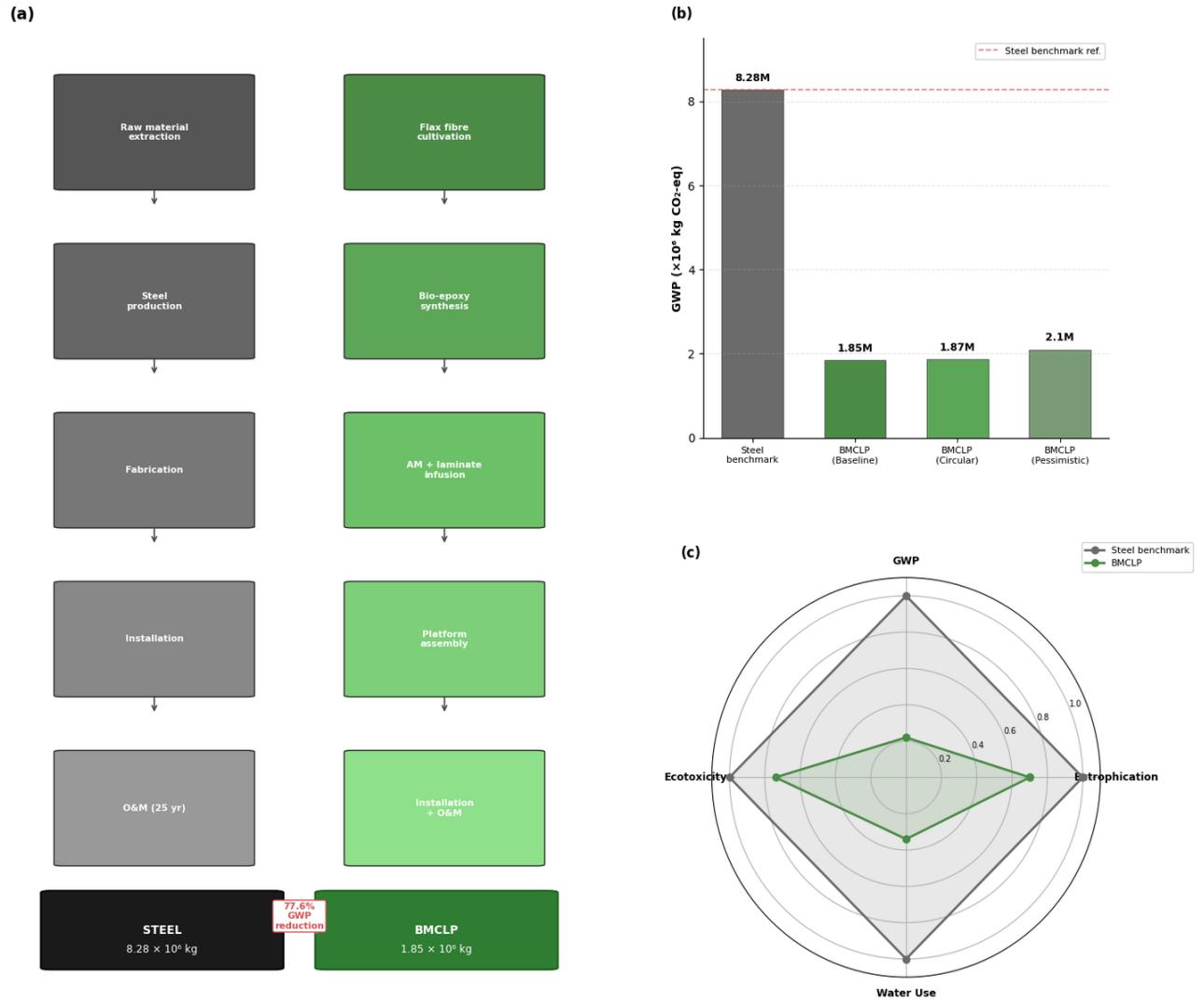

Figure 6. Circularity assessment: (**a**) material flow diagram for steel benchmark and BMCLP with end-of-life scenarios; (**b**) GWP comparison for baseline, pessimistic and circular end-of-life conditions; (**c**) radar chart of normalised life cycle trade-offs.

LCOE Sensitivity. The mass reduction led to an estimated 12–15% reduction in tow-out and heavy-lift installation costs. But the current cost of bio-epoxy resins (2.5–3.0 × petrochemical epoxy) offsets this benefit to some extent. The tornado sensitivity analysis demonstrated that the main GWP sensitivities were the bio-resin transport distance (±12% GWP variation), lattice relative density (±18%), end-of-life recycling rate (±15%) and flax yield variation (±8%) (**Figure 7**).

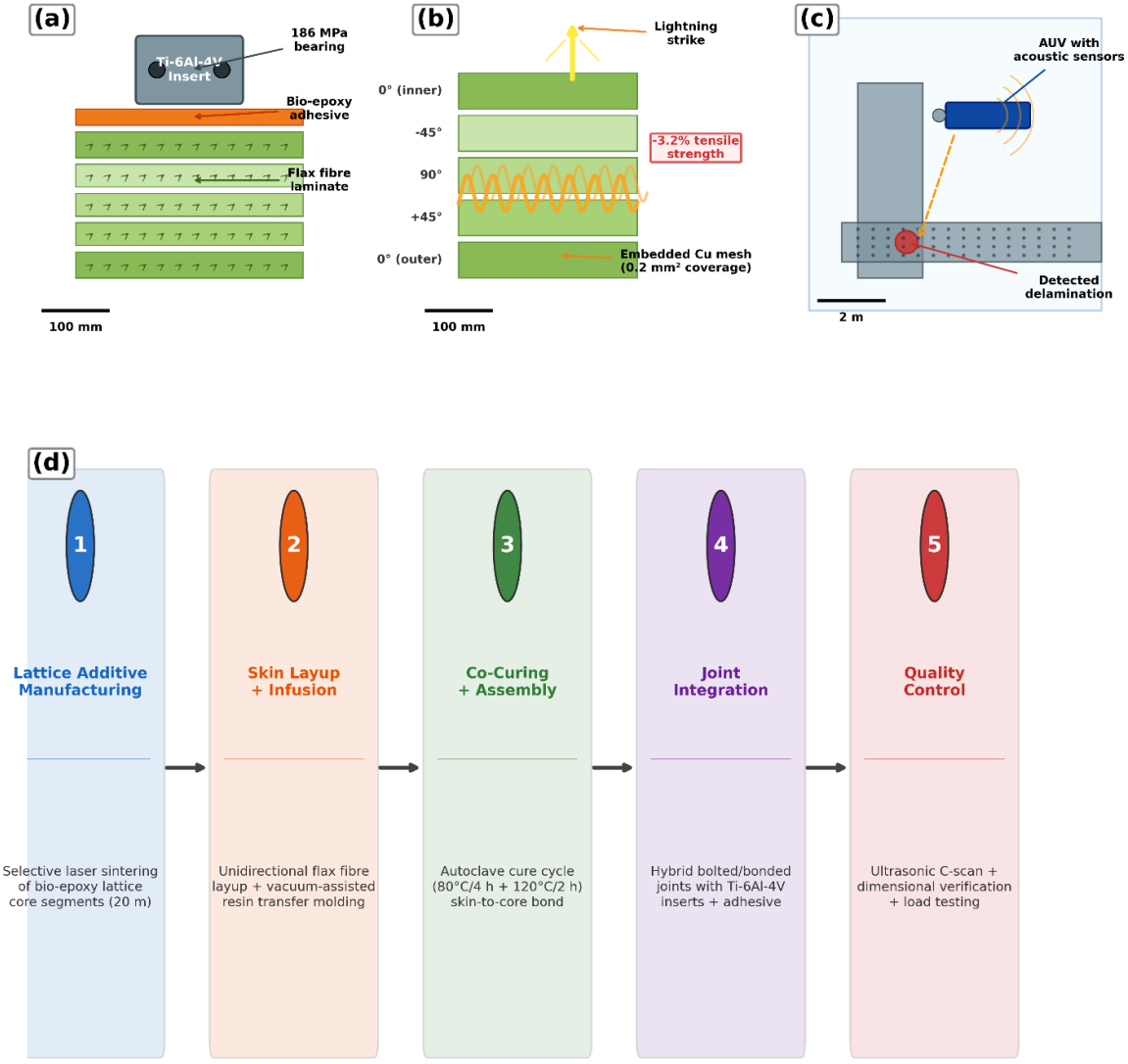

Figure 7. Manufacturing and operational details: (**a**) hybrid bolted/bonded joint cross-section with titanium insert and bio-epoxy adhesive; (**b**) lightning protection system with embedded copper mesh; (**c**) AUV inspection protocol with acoustic emission detection; (**d**) five-stage manufacturing sequence from lattice additive manufacturing to quality control inspection.

3.6. Manufacturability and Operational Reality

The hybrid bolted/bonded joint with titanium inserts reached a bearing strength of 186 MPa, satisfying the DNV-ST-C501 [12] requirements for primary composite connections. The intumescent coating applied to the flax/epoxy laminates was subjected to fire resistance tests and it was found that the coating maintained its integrity for 92 min when exposed to ISO 834 heating, which is sufficient for emergency evacuation procedures.

Coupon tests on the embedded copper lightning mesh showed a localised tensile strength reduction of 3.2%, which was confirmed by numerical sub-model predictions. The proposed inspection protocol was validated in tank trials, using underwater acoustic emission monitoring, to successfully detect simulated delamination patches (50 mm diameter).

3.7. Limitations

There are some limitations of this study that should be openly revealed. First, the hydrodynamic validation was based on equivalent Morison modelling calibrated

against published Response Amplitude Operator (RAO) data rather than direct Computational Fluid Dynamics (CFD) or wave-basin experiments, and higher-fidelity validation is recommended before full-scale deployment. Second, the long-term seawater degradation model is a Fickian diffusion model with a diffusion coefficient extrapolated from short-term immersion data. Actual field degradation may include non-Fickian behaviour, microbial attack and ultraviolet-induced surface ageing not fully captured herein. Third, additive manufacturing of 20 m lattice segments is still pre-commercial and the geometric fidelity, porosity control and production rates used in this analysis need to be demonstrated at full scale. Fourth, the LCA uses proxy inventory data sets for epoxidised linseed oil resins and solvolysis end-of-life processes due to the lack of primary industrial-scale data available for these emerging supply chains. Fifth, the fatigue S-N curve was obtained by knock-down from glass/vinyl ester baselines rather than direct experimental characterisation; long-term fatigue testing of bio-composite marine details is urgently needed to reduce this uncertainty.

3.8. Synthesis

The BMCLP demonstrates that biomimetic meta-material design with validated multi-physics assessment and circular material strategies can offer concurrent improvements of structural efficiency and environmental performance. The 68.5% mass reduction and 77.6% GWP reduction are substantial improvements over conventional steel platforms. The 18% pitch response advantage, although degraded by marine fouling, validates the concept that lattice porosity can be designed for hydrodynamic advantage. The conservative fatigue margins and predicted 78.8% residual strength at 25 years are supportive of preliminary design feasibility, subject to the limitations noted above.

4. Conclusions

The present study proposes and evaluates a bio-inspired meta-composite lattice platform (BMCLP) for floating offshore wind turbines. Principal findings are as follows:

1. The BMCLP resulted in a 68.5% reduction in structural mass compared to conventional steel semi-submersibles, enabled by topology-optimized lattice geometries and low-density bio-composite materials. The sensitivity analysis of marine growth indicated that the 18% advantage in pitch response in clean conditions was reduced to 10% with 50 mm fouling and 5% with 100 mm fouling. This highlights the importance of proactive biofouling management.
2. Spectral fatigue analysis showed that the pontoon-to-column joint was the governing joint for platform fatigue life. Damage index was 9.5×10^{-5} in 25 years and utilisation ratio was 0.277 with respect to the conservative allowable. Utilisation ratio was well below unity even with the S-N knock-down for natural fibre composites.
3. Fickian seawater degradation modelling predicted 78.8% residual compressive strength at 25 years, maintaining a margin above the 130 MPa design allowable. It was estimated to take about 18 years to reach moisture saturation.
4. Life cycle assessment showed a 77.6% reduction in the global warming potential under the baseline end-of-life conditions, due to bio-based material substitution, avoided steel production, and reduced installation energy. The trade-offs between water use and eutrophication show the importance of sustainable sourcing in agriculture.

Together, the findings support the conclusion that biomimetic meta-material design provides a structurally efficient, fatigue-durable, and environmentally responsible path to next-generation floating offshore wind infrastructure. Future research should focus on full-scale manufacturing demonstrations, long-term field exposure studies, direct fatigue characterisation of bio-composite marine details and wave-basin hydrodynamic validation.

Author Contributions

Conceptualization, K.M. and R.J.; methodology, K.M. and R.J.; software, K.M., R.J. and K.S.; validation, R.J., K.S. and S.K.S.; formal analysis, K.M. and R.J.; investigation,

K.M., R.J. and S.K.S.; resources, S.K.S. and J.N.J.; data curation, K.M. and R.J.; writing—original draft preparation, K.M.; writing—review and editing, R.J. and J.N.J.; visualization, K.M. and K.S.; supervision, J.N.J.; project administration, J.N.J.; funding acquisition, J.N.J. All authors have read and agreed to the published version of the manuscript.

Funding

This work was independently funded by the authors. No external funding was received for this research.

Institutional Review Board Statement

Not applicable.

Informed Consent Statement

Not applicable.

Data Availability Statement

The datasets generated and analyzed during the current study are available from the corresponding author upon reasonable request.

Conflicts of Interest

The authors declare no conflict of interest.

AI Use Statement

The authors declare that no artificial intelligence (AI) tools were used in the preparation of this manuscript.

References

[1] McCoy, A., Musial, W., Hammond, R., et al., 2024. Offshore Wind Market Report: 2024 Edition. National Renewable Energy Laboratory (NREL), Golden, CO, USA.

[2] Yi, Y., Zhu, D., Guo, S., et al., 2020. A review on the deterioration and approaches to enhance the durability of concrete in the marine environment. Cement and Concrete Composites. 113, 103695. DOI: https://doi.org/10.1016/j.cemconcomp.2020.103695

[3] Annamalaisamy Sannasiraj, R.D., Shi, S., Liu, X., et al., 2025. A fully coupled depth-dependent corrosion model for reinforced concrete piles under marine environmental conditions. Construction and Building Materials, 472, 140795. DOI: https://doi.org/10.1016/j.conbuildmat.2025.140795

[4] Stranddorf, L., Ladenburg, J., Rönnblom, A., et al., 2025. Evaluating environmental impacts and public preferences in offshore wind farm decommissioning. Environmental Impact Assessment Review. 118, 108253.

[5] Kappenthuler, S., Seeger, S., 2021. Holistic evaluation of the suitability of metal alloys for sustainable marine construction from a technical, economic and availability perspective. Ocean Engineering. 219, 108378. DOI: https://doi.org/10.1016/j.oceaneng.2020.108378

[6] Mohammad, S.I., Qrain, B.A., Alenazi, S.A., et al., 2025. Lifecycle Cost Management for Offshore Marine Renewable Energy Wind Infrastructure: An Integrated Model Using Circular Economy Principles. Sustainable Marine Structures. 7(3), 248–270.

[7] Napte, K.E., Kondhalkar, G., Vishal Patil, S.V., et al., 2025. Recent advances in sustainable concrete and steel alternatives for marine infrastructure. Sustainable Marine Structures. 7(2), 107–131. DOI: https://doi.org/10.36956/sms.v7i2.2072

[8] Santivongskul, P., Fox, K., Tran, P., 2025. Microstructural hierarchy of Euplectella aspergillum: Mechanical insights and biomimetic applications. Bioinspiration & Biomimetics. 20(5).

[9] Zadpoor, A.A., Mirzaali, M.J., Valdevit, L., et al., 2023. Design, material, function, and fabrication of metamaterials. APL Materials. 11(2), 020401. DOI: https://doi.org/10.1063/5.0144454

[10] Dutta, G.S., Meiners, D., Gunkelmann, N., 2023. A study of free-form shape rationalization using biomimicry as inspiration. Polymers. 15(11), 2466. DOI: https://doi.org/10.3390/polym15112466

[11] Morales, C., Claure, G., Emparanza, A.R., et al., 2020. Durability of GFRP reinforcing bars in seawater concrete. Construction and Building Materials. 270, 121492. DOI: https://doi.org/10.1016/j.conbuildmat.2020.121492

[12] DNV-ST-C501. 2022. Composite Components.

[13] Kristiansen, T., Mentzoni, F., Molin, B., 2025. The role of plate-end separation and plate thickness of perforated plates in oscillatory flow. Physics of Fluids. 37(9), 097117.

[14] Cejuela, E., Negro, V., del Campo, J.M., 2020. Evalu-

ation and optimization of the life cycle in maritime works. Sustainability. 12(11), 4524. DOI: https://doi.org/10.3390/su12114524

[15] Xiao, Y., Fani, N., Tavangarian, F., et al., 2024. Nested structure role in the mechanical response of spicule inspired fibers. Bioinspiration & Biomimetics. 19(4).

[16] He, J., Men, X., Jiao, B., et al., 2024. Coupled Aero–Hydrodynamic Analysis in Floating Offshore Wind Turbines: A Review of Numerical and Experimental Methodologies. Journal of Marine Science and Engineering. 12(12), 2205. DOI: https://doi.org/10.3390/jmse12122205

[17] Xu, M., Sitnikova, E., Li, S., 2024. A failure criterion for genuinely orthotropic materials and integration of a series of criteria for materials of different degrees of anisotropy. Royal Society Open Science. 11(5), 240205. DOI: https://doi.org/10.1098/rsos.240205

[18] Amouzadrad, P., Mohapatra, S.C., Guedes Soares, C., 2025. Numerical model for the hydroelastic response of a moored articulated floating platform with a flap-type wave energy converter. Journal of Ocean Engineering and Marine Energy. 12(2), 697–715. DOI: https://doi.org/10.1007/s40722-025-00458-x

[19] Amouzadrad, P., Mohapatra, S.C., Guedes Soares, C., 2026. Analytical and numerical model on the hydroelastic response of an array of moored circular offshore floating platforms. Ocean Engineering. 343(Part 2), 123316. DOI: https://doi.org/10.1016/j.oceaneng.2025.123316

[20] Cao, J., Li, A., Gu, C., et al., 2024. Water wave interaction with a bottom-standing surface-piercing porous compound coaxial cylinder. Physics of Fluids. 36(11), 117108. DOI: https://doi.org/10.1063/5.0235063

[21] DNV-RP-C203. 2024. Fatigue Design of Offshore Steel Structures.

[22] Peng, J., Mao, M., Xia, M., 2024. Wave Spectra Analysis on the Spatiotemporal Variability of Sea States under Distinct Typhoon Tracks in a Semienclosed Sea. Journal of Physical Oceanography. 54(3), 783–807. DOI: https://doi.org/10.1175/JPO-D-23-0066.1

[23] Baley, C., Davies, P., Troalen, W., et al., 2024. Sustainable polymer composite marine structures: Developments and challenges. Progress in Materials Science. 145, 101307. DOI: https://doi.org/10.1016/j.pmatsci.2024.101307

[24] Chamley, A., Baley, C., Gayet, N., et al., 2024. (Bio)degradation of biopolymer and biocomposite in deep-sea environments. Marine Pollution Bulletin. 209(Part B), 117230. DOI: https://doi.org/10.1016/j.marpolbul.2024.117230

[25] Krishnamurti, R., 2025. Life Cycle Cost Analysis, Sustainability, and the Circular Economy: Stainless Steel as a Material for Future-Ready Infrastructure. In Proceedings of the Conference Series on Sustainable Architecture Circular Economy (SACE 2025), New Delhi, India, 4–5 March 2025.

[26] Stranddorf, L., Ladenburg, J., Zuch, M., 2026. Tipping the decision of offshore wind farm decommissioning—The causal effects of biodiversity illustrations and information. Ecological Economics. 239, 108796.

[27] Zhou, T., Hu, C., 2025. A review on life-cycle cost analysis of anticorrosion coating systems relevance to its economic evaluation and performance insights for the structures in marine and offshore environment. Anti-Corrosion Methods and Materials. 73(2), 297–315.

[28] Darling, H., Schmidt, D.P., Xie, S., et al., 2024. OC6 Phase IV: Validation of CFD Models for Stiesdal TetraSpar Floating Offshore Wind Platform. Wind Energy. 28(1), e2966. DOI: https://doi.org/10.1002/we.2966

[29] Ashby, M.F., Bréchet, Y.J.M., 2003. Designing hybrid materials. Acta Materialia. 51(19), 5801–5821. DOI: https://doi.org/10.1016/S1359-6454(03)00441-5

[30] Collino, R.R., Ray, T.R., Fleming, R.C., et al., 2016. Deposition of ordered two-phase materials using microfluidic print nozzles with acoustic focusing. Extreme Mechanics Letters, 8, 96–106. DOI: https://doi.org/10.1016/j.eml.2016.04.003

[31] Amouzadrad, P., Mohapatra, S.C., Guedes Soares, C., 2025. Review on sensitivity and uncertainty analysis of hydrodynamic and hydroelastic responses of floating offshore structures. Journal of Marine Science and Engineering. 13(6), 1015. DOI: https://doi.org/10.3390/jmse13061015

[32] Bergua, R., Wiley, W., Robertson, A., et al., 2024. OC6 project Phase IV: Validation of numerical models for novel floating offshore wind support structures. Wind Energy Science. 9(4), 1025–1051. DOI: https://doi.org/10.5194/wes-9-1025-2024